

Supply-limited bedform patterns and scaling downstream of a gravel–sand transition

JEREMY G. VENDITTI*† , JEFFREY A. NITTROUER‡ , MEAD A. ALLISON§¶ ,
ROBERT P. HUMPHRIES** and MICHAEL CHURCH††

*Department of Geography, Simon Fraser University, Burnaby, BC, V5A 1S6, Canada
(E-mail: jeremy_venditti@sfu.ca)

†School of Environmental Science, Simon Fraser University, Burnaby, BC, V5A 1S6, Canada

‡Department of Earth, Environmental and Planetary Sciences, Rice University, Houston, TX 77005, USA

§Department of Earth and Environmental Sciences, Tulane University, New Orleans, LA 70118, USA

¶The Water Institute of the Gulf, Baton Rouge, LA 70825, USA

**Golder Associates Inc., Redmond, WA 98052, USA

††Department of Geography, The University of British Columbia, Vancouver, BC, V6T 1Z2, Canada

Associate Editor – Charlie Bristow

ABSTRACT

A distinct suite of sand bedforms has been observed to occur in laboratory flows with limited sand supply. As sand supply to the bed progressively increases one observes sand ribbons, discrete barchans and, eventually, channel spanning dunes; but there are relatively few observations of this sequence from natural river channels. Furthermore, there are few observations of transitions from limited sand supply to abundant supply in the field. Bedforms developed under limited, but increasing, sand supply downstream of the abrupt gravel–sand transition in the Fraser River, British Columbia, are examined using multi-beam swath-bathymetry obtained at high flow. This is an ideal location to study supply-limited bedforms because, due to a break in river slope, sand transitions from washload upstream of the gravel–sand transition to bed material load downstream. Immediately downstream, barchanoid and isolated dunes are observed. Most of the bedform field has gaps in the troughs, consistent with sand moving over a flat immobile or weakly mobile gravel bed. Linear, alongstream bedform fields (trains of transverse dunes formed on locally thick, linear deposits of sand) exhibit characteristics of sand ribbons with superimposed bedforms. Further downstream, channel spanning dunes develop where the bed is composed entirely of sand. Depth scaling of the dunes does not emerge in this data set. Only where the channel has accumulated abundant sand on the bed do the dunes exhibit scaling congruent with previous data compilations. The observations suggest that sediment supply plays an important, but often overlooked, role in bedform scaling in rivers.

Keywords Fluvial dunes, Fraser River, sand bedforms, supply-limited bedforms.

INTRODUCTION

Sand bedforms in river channels dominate sediment transport processes and flow resistance. They also leave signatures in the subsurface that

are used to infer palaeohydraulics. There have been relatively few observations in rivers of sand bedforms developed under conditions of limited sand supply, notable exceptions being McCulloch & Janda (1964) and Carling *et al.*

(2000). Yet such features are common through gravel–sand transitions (GST) and in many locations downstream of dams where sand-sized sediment is impounded. In aeolian environments, bedforms developed under low rates of sand supply, including barchan and crescentric dunes, are well-documented (Bagnold, 1941; Lancaster, 1995). Bedforms with limited sand supply have also been identified in tidal marine environments (Allen, 1968; Carling *et al.*, 2005; Ernstsens *et al.*, 2005; Williams *et al.*, 2006) and on the sea floor (Kenyon & Stride, 1967; Lonsdale & Malfait, 1974; Lonsdale & Spiess, 1977; Wynn *et al.*, 2002; Franzetti *et al.*, 2013), suggesting that a distinctive suite of bedforms develops under sediment supply-limited conditions in many flow environments at Earth’s surface.

The term ‘sediment supply limited’ is applied uncritically in the sediment transport literature. It is typically thought of as a situation where the supply of sediment to a river reach is less than the capacity to transport it. If the transport capacity exceeds the sediment supply to the channel for long periods of time, the channel will become non-alluvial, with periodically exposed bedrock. If a river is to remain alluvial in the long-term, river morphology, bed surface grain size and gradient must adjust to pass the water and sediment load. So, for an alluvial river, the conditions where sediment supply is less than capacity conditions must be either temporary, occurring between sediment supply events, or an interim condition occurring while a river evolves to a new equilibrium condition. Supply limitation may also refer to a condition where the capacity to transport a particular grain size exists, but the size is not available in the supply, leaving the bed material depleted in a particular size. Within this context, the term ‘supply limited’ has been applied to bimodal sand and gravel in which the sand supply, from upstream and/or from below a surficial gravel armour, is insufficient to render the bed entirely sand. In this sense, the supply limitation refers to a condition where the supply of sand is insufficient to cover the bed entirely with sand. The supply limitation to the bed might be the consequence of limited amounts of sand transported into a reach with an otherwise coarser bed, or a generous supply, most of which is immediately advected onward and not lying on the bed. Use of the term ‘supply limited’ herein is consistent with this condition, where the supply of sand is not sufficient to completely cover

an otherwise coarser bed, regardless of how the limitation occurs.

Experimental work has shown that, in the circumstance just described, a well-defined sequence of sand bedforms develops over otherwise immobile gravel beds as the supply rate of sand is increased (cf. Hersen *et al.*, 2002; Kleinhans *et al.*, 2002; Tuijnder *et al.*, 2009; Tuijnder & Ribberink, 2012; Grams & Wilcock, 2014; Venditti *et al.*, 2017). Figure 1 is a conceptual model developed by Kleinhans *et al.* (2002) which shows that, as sediment supply increases, the following bedforms emerge sequentially: (i) sand ribbons; (ii) individual barchan-shaped dunes; and (iii) channel spanning dunes. Gravel may become locally mobile in the largest dune troughs as intense turbulence winnows sand from below the mobile armour layer. In laboratories, the sequence is controlled by transport stage, given by the Shields number:

$$\tau^* = \frac{\tau}{(\rho_s - \rho)gD} \quad (1)$$

where τ is the grain-related shear stress, ρ_s and ρ are the sediment and water densities, g is gravitational acceleration and D is a characteristic grain-size. At low transport stages ($0.01 < \tau^* < 0.05$), just above the threshold for motion of the sand, sand ribbons grade to low-amplitude, elongated barchans with superimposed bedforms developing with increasing sand supply to the bed. At moderate transport stages ($0.05 < \tau^* < 0.5$), the bed grades from sand-ribbons to small barchans to dunes while at higher transport stages ($0.5 < \tau^* < 1.0$), barchans grade to dunes with increasing sediment supply (Kleinhans *et al.*, 2002). The overlapping ranges are mediated by sediment supply, with the sequence sand ribbons to dunes advancing at lower values of τ^* with the increase of sand supply.

Most previous work on this sequence of supply-limited sand bedforms has been done in flume channels where flow conditions are steady and uniform, a rare condition in natural channels. There is a paucity of high resolution observations and thus supporting information from river channels is lacking. The lack of field observations of this sequence of bedforms is linked to the dynamic behaviour of sediment transport in natural channels. Sediment supply gradients typically occur over long distances in rivers (cf. Nittrouer *et al.*, 2011; Nittrouer, 2013). Sediment supply can also vary temporally during flood flow events, producing a sediment supply-limited sequence

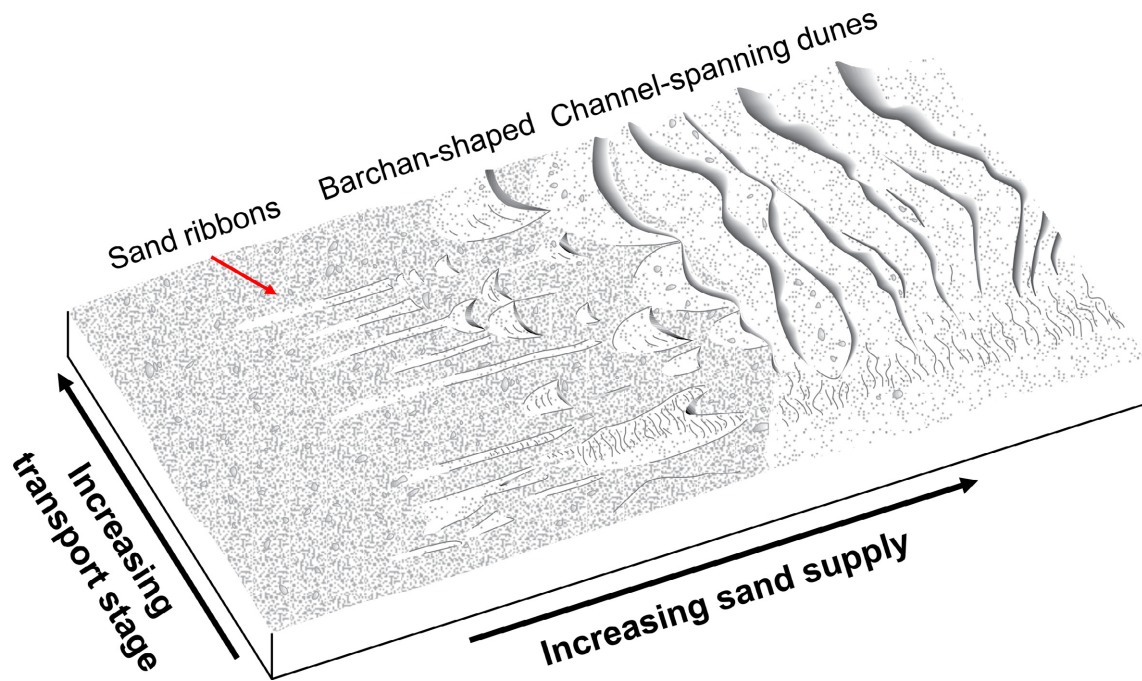


Fig. 1. Conceptual model for sandy bedform development over an immobile gravel bed. Flow is from left to right. Modified from Kleinhans *et al.* (2002).

through time at a particular location in a river. Obtaining measurements to illustrate and analyze the effects of a limited sediment supply is, then, logistically difficult because they need to be taken over long distances and/or timed with a hydrograph. However, the sediment supply changes that occur through a gravel–sand transition (GST) provide an opportunity to study this bedform sequence in natural channels. Here, observations are presented of bedforms through the ‘diffuse extension’ of the GST in the Fraser River (Venditti & Church, 2014; Venditti *et al.*, 2015) during flood flow conditions. The diffuse extension is the reach beyond the arrested gravel front (*sensu* Parker & Cui, 1998) in which some fine gravel continues to be transported and deposited in the thalweg and on bar heads, in places forming a light armour over which sand, now the dominant portion of the bedload, passes. In the Fraser River, the diffuse extension continues for many kilometres beyond the gravel front.

The sand bed develops by deposition of a large portion of the suspended sand load within the first kilometre beyond the main gravel front due to the break in water surface gradient and consequent decline in shear stress, immediately upstream. Sand accumulates here during low and intermediate freshets and is redistributed downstream at high flows to form the sand bed

in the distal reach of the river. Late in high flow events, when little additional sand is being supplied from upstream, the sand store immediately below the GST may approach exhaustion and the bedform suite associated with limited sand supply then develops in the succeeding 15 km. The morphology and scaling of bedforms through this reach are examined. The specific questions addressed in this study are: (i) do bedform patterns conform with increasing sediment supply to the bed; (ii) do dunes conform to conventional depth-scaling through the GST; and (iii) what controls the height and length of supply-limited dunes?

METHODS

Field Site

The Fraser River drains 228 000 km² of the central interior of British Columbia. The river flows through a 390 km long sequence of bedrock canyons and emerges from the mountain front at Hope, British Columbia (Canada) as an alluvial channel. Figure 2 summarizes the downstream changes in topography, hydraulics and sediment characteristics that occur through the alluvial reach of the river as it approaches the ocean.

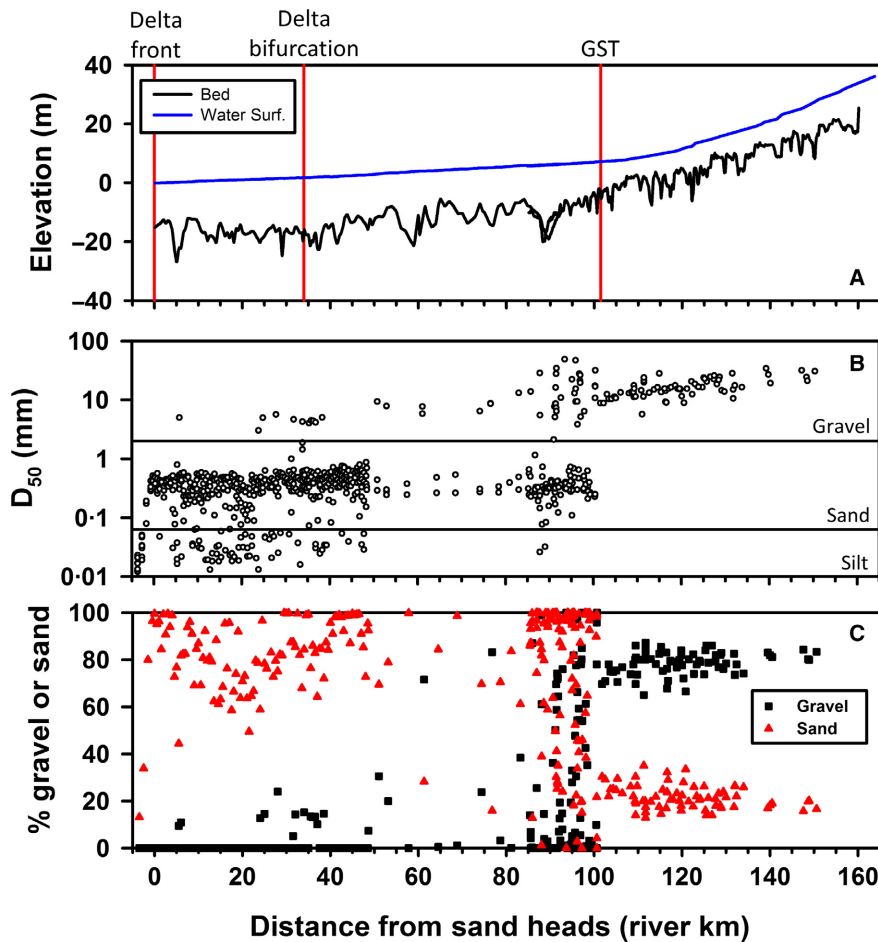


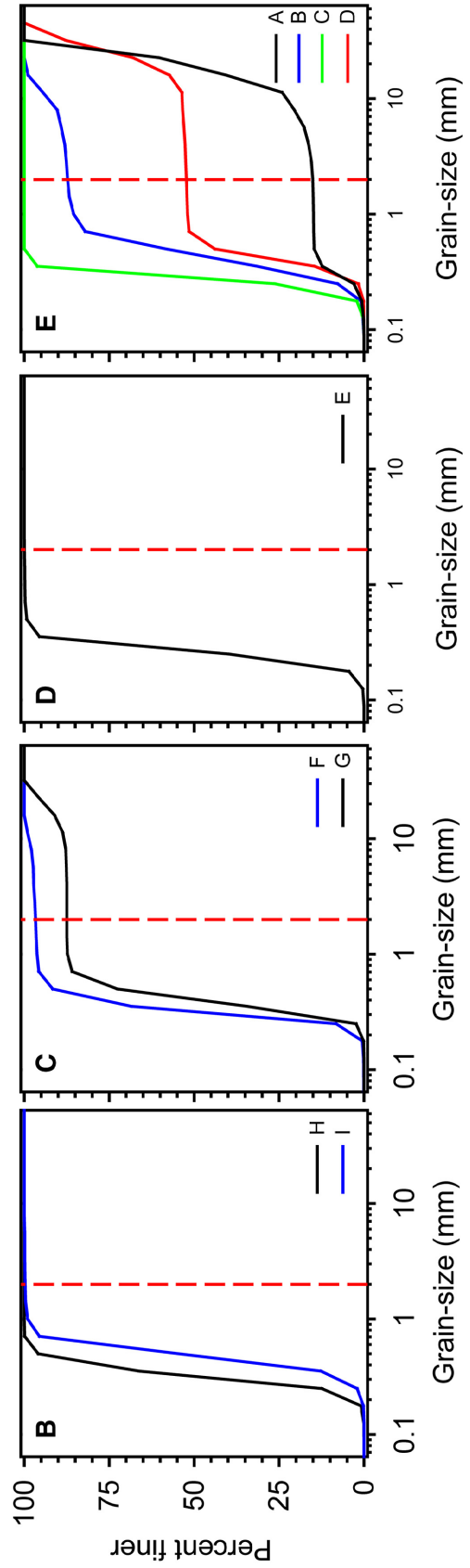
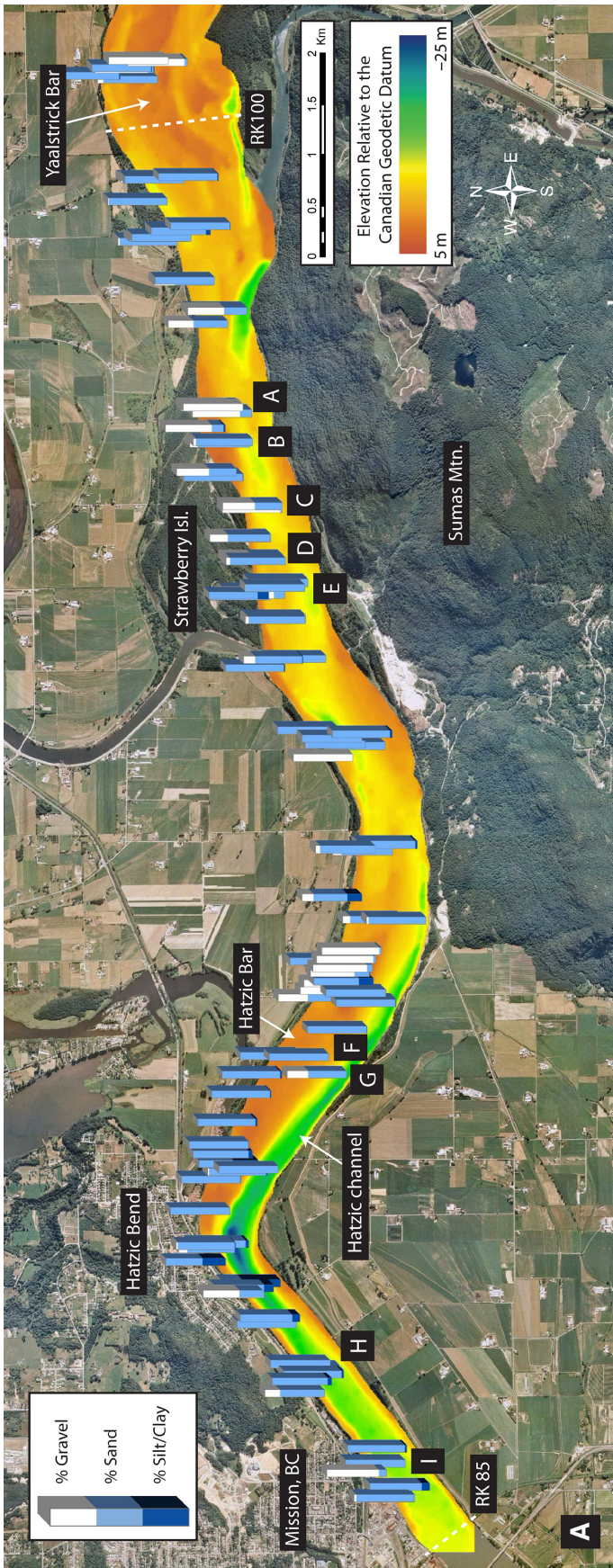
Fig. 2. Downstream change in: (A) water surface and bed elevation; (B) median grain size (D_{50}); (C) percent sand and gravel in the Fraser River as it approaches the ocean at Sand Heads.

The alluvial portion of the river takes the form of a wedge of gravel and cobble material between RK 160 to RK 90, with a break in bed slope at RK 90 (Fig. 2A). There is a break in the water surface gradient at RK 102, upstream of the break in bed slope, that gives rise to a grain-size transition from gravel to sand (Fig. 2B).

The river is gravel-bedded from Hope, BC (RK 160) to RK 100.5 (Fig. 2B) (Venditti & Church,

2014) (RK is river kilometres measured upstream from the river mouth at the Strait of Georgia). The bed material is framework supported 80 to 90% gravel and 10 to 20% sand (McLean *et al.*, 1999) and the subsurface median grain size fines from *ca* 30 to *ca* 10 mm downstream (McLean *et al.*, 1999; Ham, 2005; Venditti & Church 2014) (Fig. 2C). The threshold for general movement of the gravel bed is *ca* 5000 m³ sec⁻¹

Fig. 3. (A) Bed material grain size through the diffuse extension of the gravel–sand transition reach in the Fraser River. Bathymetric data collected during a 2008 freshet survey by Public Works and Government Services, Canada (details of survey in Venditti & Church, 2014). Each tricolour (dark blue, light blue and white) bar represents one bed material sample. The proportion of a colour on the bar indicates the percent of the sample composed of a particular size class. For example, the tricolour bar in the legend is 33.3% gravel, 33.3% sand and 33.3% silt/clay. Capital letters ‘A’ to ‘H’ correspond to grain-size distributions in panels (B) to (E). Interpretations from MBES data indicate that the bed is: flat at ‘A’, composed of dunes with gaps in the troughs at ‘B’, ‘C’ and ‘D’, and an along-stream dune field at ‘E’. ‘F’ and ‘G’ are from Hatzic Bar and Channel, respectively. ‘H’ is from a large dune field developed on a bar downstream of Hatzic Bend and ‘I’ is from a superimposed dune field. Panel (A) is modified from Venditti & Church (2014).



(McLean *et al.*, 1999), which is exceeded annually. Sand is carried as washload through the gravel-bedded portion of the river at flows that move the gravel bed [following Church (2005), washload moves in continuous suspension and commonly constitutes <10% of the bed]. Hence sand is generally absent on the surface in the main channel upstream from the GST at RK 100.5. During low freshets and on waning flows, sand is deposited in the gravel reach in side channels, and on bar surfaces. During high freshets, the stored sand is flushed out of the gravel-bedded reach of the river to the sand-bedded reach (McLean *et al.*, 1999). What exactly constitutes ‘low’ and ‘high’ freshets with respect to this process is not currently known but sand accumulation has been observed during freshets much below the mean annual flood flow ($8766 \text{ m}^3 \text{ sec}^{-1}$) and bed elevations in backwater channels decline notably during exceptional flood flows ($>10\,000 \text{ m}^3 \text{ sec}^{-1}$) (McLean, 1990; Ham, 2005).

The GST takes the form of an arrested gravel front that terminates abruptly at RK 100.5 and is coincident with a break in flood water surface gradient (Venditti & Church, 2014). Downstream of RK 100.5, the bed material is sand (Fig. 2B), although some significant bimodal, matrix-supported, sand–gravel deposits occur in some of the pools, along portions of the thalweg and on the proximal bar surfaces. This pattern is highlighted in Fig. 3, which shows the composition of individual samples collected through the 15 km reach immediately downstream of the abrupt transition in 2007 and 2008 (see Venditti & Church, 2014). This reach is the proximal portion of the diffuse extension of the GST and grain-size distributions close to the gravel front are a mix of sand, bimodal sand–gravel and gravel (Fig. 3A and E), but the vast majority of samples are sand (Fig. 3A). Venditti *et al.* (2015) showed that gravel movement does not generally occur in the reach, although small amounts are transported over the sand due to particle exposure on the bed, resulting in the patterns shown in Fig. 3A. Moving downstream, that gravel mode disappears until the bed is almost entirely sand bedded by RK 85 (Fig. 3A).

In the sand-bed reach, sand is carried as suspended bed material load and as bedload in the form of migrating dunes. The bed material – washload size division is *ca* 0.180 mm (McLean *et al.*, 1999; Attard *et al.*, 2014). Sand on the bed throughout the sand-bedded reach of the river and the main delta distributary channel

has a $D_{50} = 0.383 \text{ mm}$ (Venditti & Church, 2014). Sand makes up 35% of the average annual suspended load at RK 85 (the balance being silt and clay), of which half – about 3 million tonnes – is bed material.

Observations

Bed topography was measured in the reach immediately downstream of main channel spanning the GST from the 7 m long *R/V Lake Itasca* from 19 to 21 June 2007 at a discharge of $8800 \text{ m}^3 \text{ sec}^{-1}$ just after the peak flow (Fig. 4) of $11\,800 \text{ m}^3 \text{ sec}^{-1}$ (return period of 12 years). Bathymetry was measured using a Reson 7101 Seabat[®] Multibeam Echosounder (MBES; Teledyne Reson PDS, Slangerup, Denmark). Positioning was accomplished using a GPS differentially corrected by the signal of a Canadian Coast Guard beacon about 85 km to the west of the study reach. The differential GPS provides positioning with an accuracy of 0.25 m horizontally and 0.50 m vertically. The manufacturer reported depth resolution of the MBES is 1.25 cm (Reson Inc., 2009). The head generates 101 equidistant beams in a swath perpendicular to the vessel track. Navigation, orientation and attitude data (heave, pitch and roll) were recorded using an Applanix POS MV V3 gyroscope inertial guidance system (Applanix, Richmond Hill, Ontario, Canada) mounted inside the vessel. Raw MBES data were imported into CARIS HIPS[®] software for post-processing where lines and soundings were merged to produce bathymetric grids. This software allows for the removal of ‘bad pings’ and corrections for changes in heave, pitch, roll and tidal stage. The data were then imported into ArcGIS[®] and gridded at 1 m for further analysis of the bed surface and measurements of bedform characteristics. The areal coverage of the MBES data is shown in Fig. 5.

In order to examine the characteristics of the bedforms, lines of bed topography oriented along the main flow path and slope of the bed were extracted from the MBES data. The lines were not randomly chosen, but rather were selected to provide spatial coverage through the bedform field so that individual bedforms were measured only once. Where the bedforms were not spatially continuous, straight lines crossed the crests perpendicularly where the bedform train was highest. The heights and lengths of 2642 bedforms were then measured from the resulting bed transects, and used to compute aspect ratio (bedform length/height). Data are aggregated into

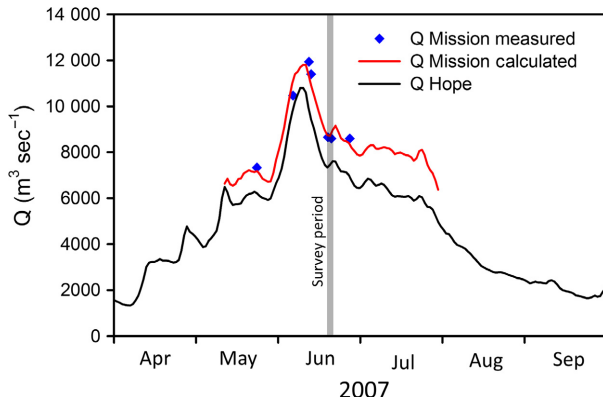


Fig. 4. Hydrographs for the Fraser River at Mission (Water Survey of Canada Station 08MH024) and Hope (WSC station 08MF005) for 2007 freshet. The WSC uses a rating curve to calculate discharge at Mission when the combined flow at Hope and the Harrison River, a tributary between Hope and Mission, exceeds $5000 \text{ m}^3 \text{ sec}^{-1}$ due to the tidal influence on water levels at low flows, limiting the length of the record. These calculations are complemented by discharge measurements by the WSC.

four sections within the reach (Fig. 5) that had bedforms with similar characteristics. The number of observations in each section is as follows: (i) Upper Transition Reach ($n = 1527$ bedforms); (ii) Hatzic Bar ($n = 513$); (iii) Hatzic Channel, adjacent to Hatzic Bar ($n = 186$); and (iv) Lower Transition Reach ($n = 416$). Hatzic Bar is a

concave-bank bench bar complex (*sensu* Hickin, 1979) that is subaerially exposed at low flows. The number of bedforms measured in each section reflects the area of the mapped channel bed as well as the size of the bedforms (for example, bigger and fewer bedforms versus smaller and more numerous bedforms).

Two velocity profiles were measured in the Upper Transition Reach and three in the Lower Transition Reach (Fig. 5), in order to characterize local velocity and shear stresses. Measurements were obtained with a 1200 kHz RDI Rio Grande Workhorse ADCP (Teledyne Reson) using bottom track as the velocity reference. Mean velocity U is a weighted depth-average. Shear velocity (u_*) is calculated from the slope (a) of a natural log-linear fit to the velocity profile as $u_* = \kappa a$, where κ is the von Karman constant (0.41). Shear stress is calculated as $\tau = \rho u_*^2$.

RESULTS

Flow and local shear stresses in the Upper Transition Reach (UTR) and Lower Transition Reach (LTR) are summarized in Table 1. Depth averaged-velocity varies considerably with location and depth; however shear velocity is generally *ca* 0.1 m sec^{-1} and shear stresses are *ca* 10 Pa in both the LTR and the UTR, except for the profile

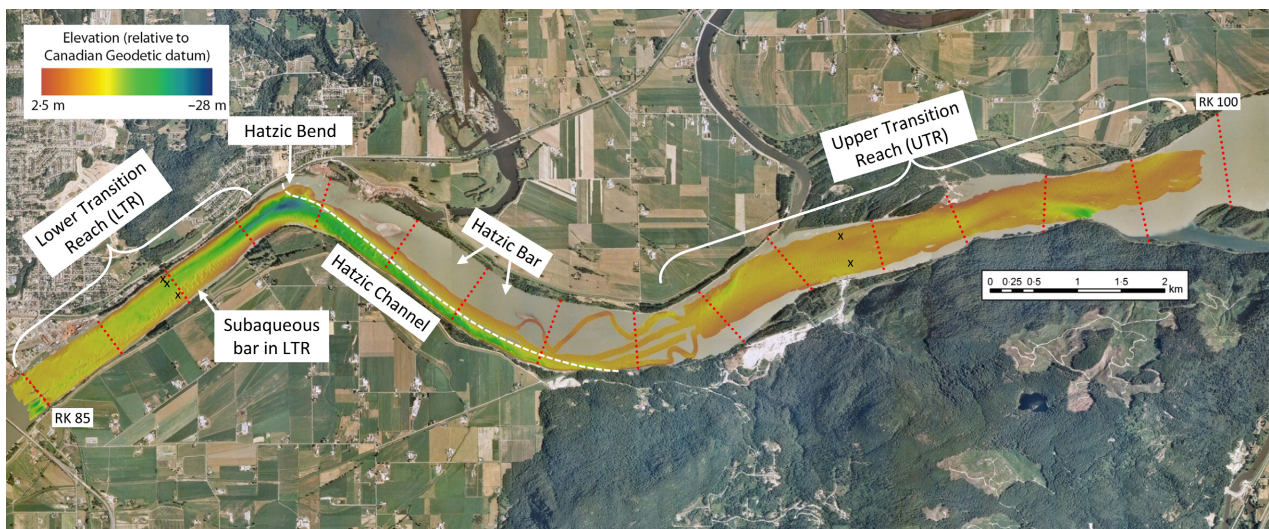


Fig. 5. Multibeam bed topography of the diffuse gravel–sand transition reach of the Fraser River. The gravel reach terminates abruptly at RK 100.5. Dashed white line separates Hatzic Channel from Hatzic bar. Red dotted lines are river kilometres (RK) measured in 1 km increments along the centreline. Black crosses (x) indicate locations of velocity profiles used to calculate summary flow data in Table 1. See Figs 6, 7, 9 and 10 for larger scale views of the bed topography.

taken in relatively shallow water along the north bank in the LTR. These shear velocity and stress values are consistent with the more detailed study of velocity and shear stresses downstream of this GST (see Venditti *et al.*, 2015). At these shear stresses, the gravel sizes present upstream of the GST (>10 mm) are only marginally mobile and the median sand size (0.383 mm) should be carried as suspended bed material load (Venditti *et al.*, 2015). Lamb & Venditti (2016) showed that rivers lose the ability to transport sand as wash-load where shear velocity drops below *ca* 0.1 m sec⁻¹. Hence the reason the diffuse extension of the GST emerges in this reach.

Bedform morphology

The UTR is mainly sand covered, but there are notable gravel patches and locations with a mixture of sand and gravel (Fig. 3A). Most of the UTR is covered by dunes with gaps in the troughs, indicating either that the dunes are migrating over a coarser, immobile bed or that substantial gravel deposits in the bedform

Table 1. Flow at select locations in the Upper Transition Reach (UTR) and Lower Transition Reach (LTR; see Fig. 5).

Profile	Location	U (m sec ⁻¹)	h (m)	u^* (m sec ⁻¹)	τ (Pa)
UTR1	North bank	1.06	9.33	0.102	10.40
UTR2	South bank	1.30	10.90	0.096	9.22
LTR1	Centre	1.78	16.40	0.101	10.20
LTR2	North bank	0.775	7.40	0.195	38.00
LTR3	South bank	1.37	11.80	0.109	11.90

troughs. Four types of bedform morphologies are observed in this area: (i) barchan and barchanoid dunes (Fig. 6A and B); (ii) individual transverse or irregular ('isolated') dunes (Fig. 6B); (iii) dune fields with gaps in the trough (Fig. 7A); and (iv) trains of transverse dunes

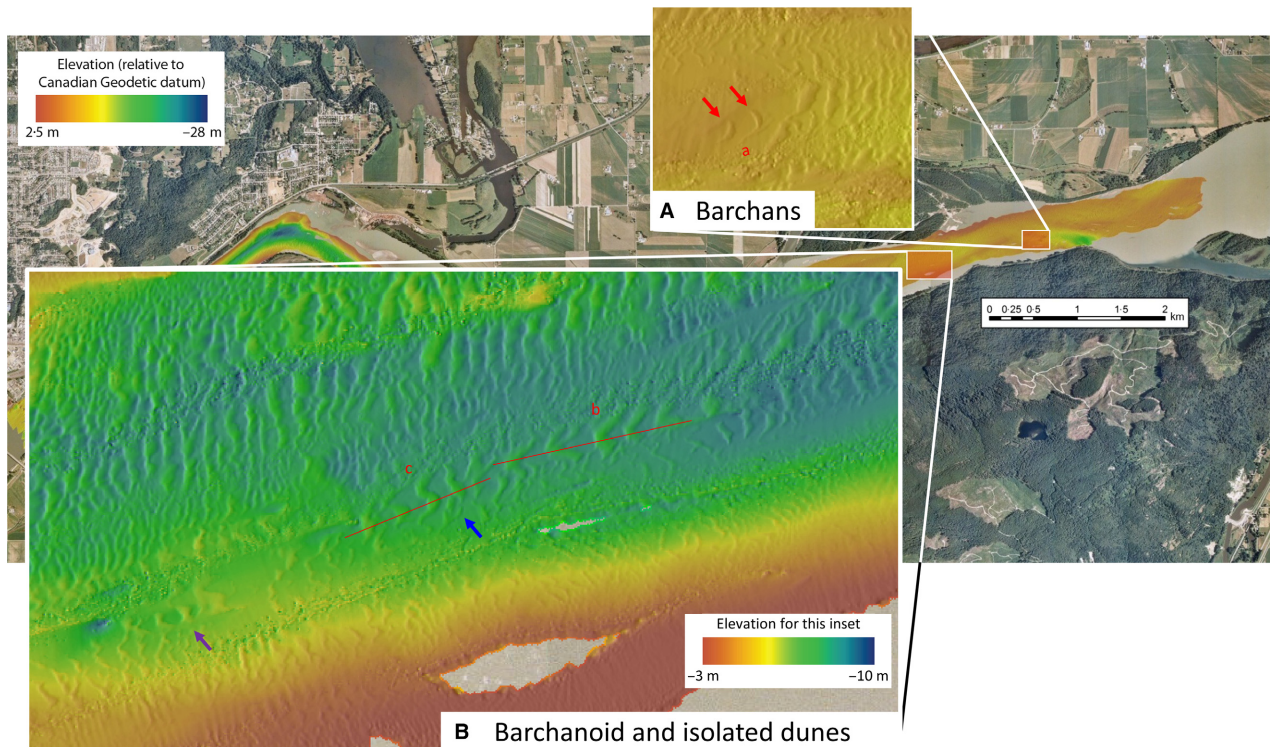


Fig. 6. (A) Barchan dunes and (B) barchanoid and isolated dunes in the Upper Transitional Reach. Red arrows highlight examples of barchan dunes. Blue arrow highlights example of a barchanoid dune field. Purple arrow highlights example of isolated dunes. Lines labelled 'b' and 'c' correspond to bedform profiles shown in Fig. 8. An unlabelled line at 'a' crosses both barchans, perpendicularly, but would obscure the features and is not shown. Elevation scale for insets are the same as the base map, unless otherwise indicated. Flow is from right to left.

formed on a locally thick, linear deposits of sand, which are referred to here as *linear, along-stream dune fields* (Fig. 7B).

Barchan dunes are common with the lateral terminations of the crest lines oriented in the downstream direction (Fig. 6A). Barchanoid dunes, resembling barchans, but imperfect in form (for example, lacking a wing or joined to another) are also common (Fig. 6B). Many of these barchan and barchanoid features are also isolated dunes, like those commonly observed in aeolian desert environments when bedforms are developed over an otherwise immobile boundary (e.g. Bagnold, 1941; Lancaster, 1995). Some barchanoid dunes are in a continuous field (Fig. 6B). Transects through the isolated barchans and barchanoid shaped dunes reveal a flat continuous surface underlying the dunes (Fig. 8A to C). Sediment samples from adjacent flat areas indicate that this is a gravel bed

(Fig. 3A and E – Sample A). The occurrence of isolated dunes is common downstream of the deeply scoured gravel-bedded pools in the channel (compare Figs 3A and 6), confirming migration of sand dunes over a coarser immobile bed.

Dunes with gaps in the troughs (Fig. 7A) also have a flat continuous surface underlying the dune field (Fig. 8D and E), indicating migration over a flat gravel bed. Sediment samples are a mixture of sand (Fig. 3A and E – Sample C) and sand with a secondary mode of gravel (Fig. 3A and E – Samples B and D). Areas can be identified where linear, alongstream dune fields occur (Fig. 8B) that are composed entirely of sand (Fig. 3D – Sample E). This indicates an area of locally continuous sand coverage that is extended in the downstream direction. Sand ribbons formed by streamlining of local accumulations of sand and superimposed by small-scale bedforms, have been observed in

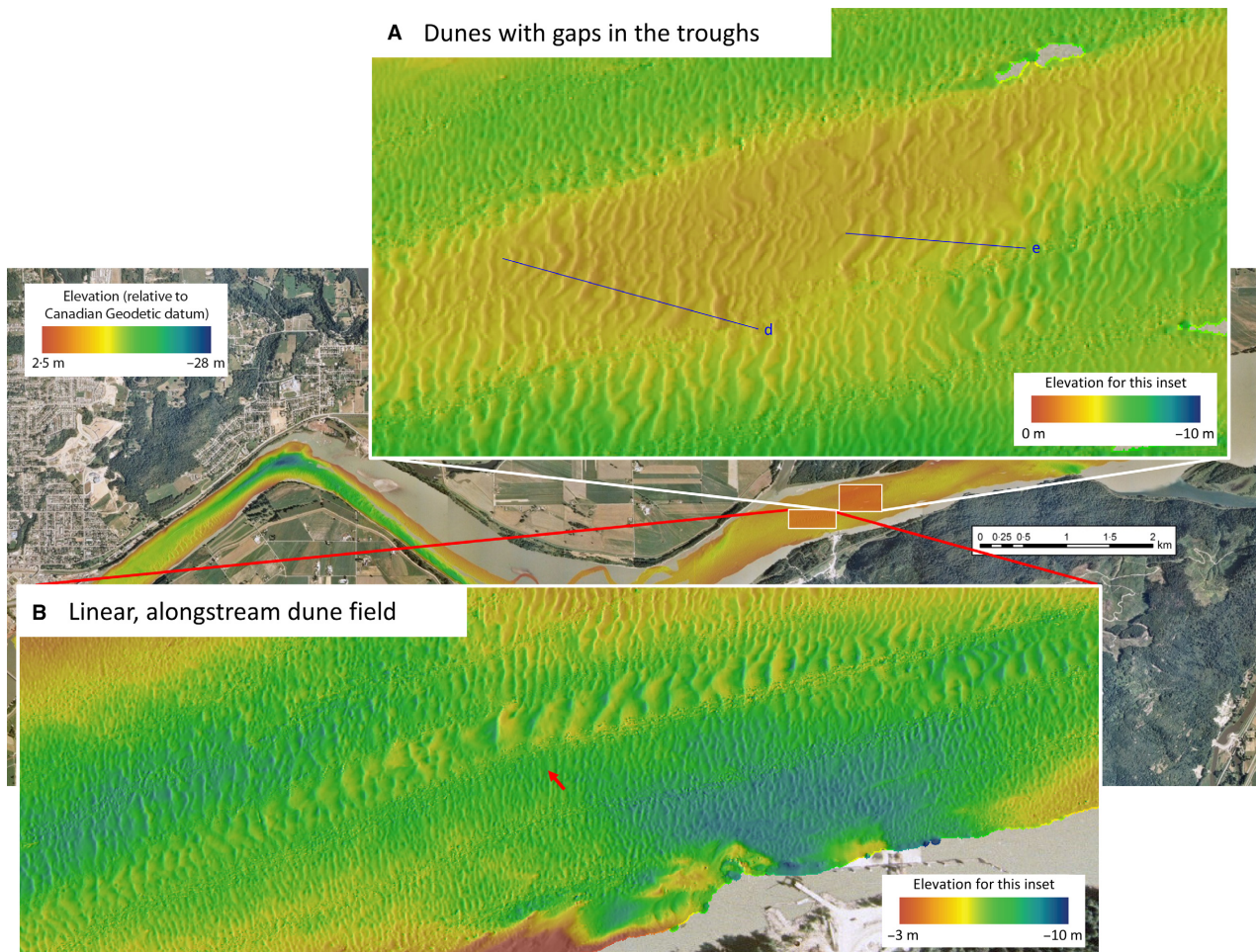


Fig. 7. (A) Dunes with gaps in troughs and (B) a linear, alongstream dune field (red arrow) in the Upper Transitional Reach of the Fraser River. The red arrow points to a linear, alongstream dune field. Lines labelled ‘d’ and ‘e’ correspond to bedform profiles shown in Fig. 8. Grey areas in (A) are gaps in data coverage. Flow is from right to left.

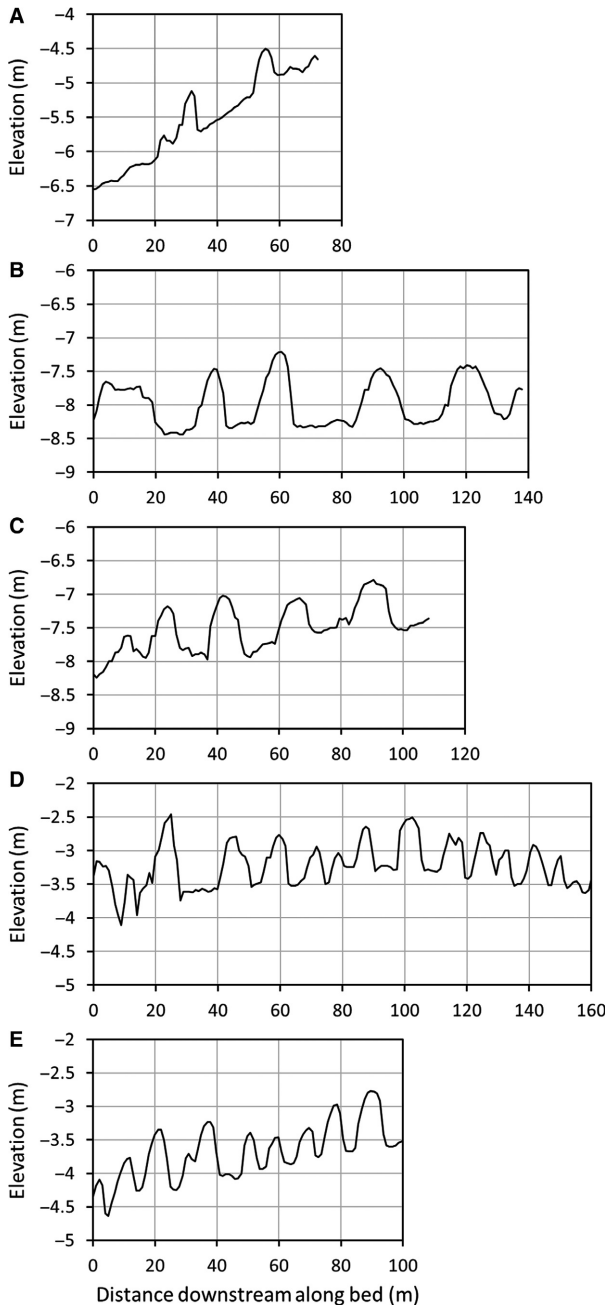


Fig. 8. Transects through: (A) isolated barchan dunes (line ‘a’ in Fig. 6A); (B) barchanoid features (line ‘b’ in Fig. 6B); (C) barchanoid features (line ‘c’ in Fig. 6B); (D) dunes with gaps in their troughs (line ‘d’ in Fig. 7A); and (E) dunes with gaps in their troughs (line ‘e’ in Fig. 7A).

laboratory experiments (cf. Kleinhans *et al.*, 2002). In this respect, alongstream dune fields are analogous to these sand ribbons, but at a larger scale.

Across the top of Hatzic Bar, the bedforms are developed on continuous sand cover (Fig. 9A)

with trace amounts of gravel in some patches (Fig. 3A and C – Sample F). There are no barchanoid shapes or linear, alongstream dune fields. The coverage of multibeam data on the bar top is limited in this study, because water depths were too shallow (<2 m) for successful operation of the MBES, but reconnaissance at low flow when the bar top was subaerially exposed indicates that the interpretation herein of laterally continuous sand cover with dunes is correct. In Hatzic Channel, which carries most of the flow adjacent to the bar, the bed changes from having small-scale bedforms typical of the UTR, to a flat bed with gravel patches, to bedforms that increase in size progressing downstream into Hatzic Bend (Fig. 9B), indicating increasing sand volume on the bed downstream. Figure 3A shows that the bed is composed of sand throughout the channel, except in the flat bed section where the sediment is a gravel–sand mixture (Fig. 3C – Sample G).

In contrast to the UTR, the LTR is entirely sand covered (Fig. 3A and B – Samples H and I), except along the north bank of the river where there is a patch of gravel (Fig. 3A). The gravel patch may not be natural because there has been extensive riprapping along the north shore to prevent bank erosion into a railway line. Flow through the Hatzic Bend forces deposition on the south side of the channel forming a large subaqueous bar (Fig. 5). The dunes on this bar are notably larger than anywhere else within the reach (Fig. 10A). The largest dunes on the bar have mean heights $H = 3.0$ m and mean lengths $L = 50$ m. Moving downstream through the LTR, the areal coverage of sand increases (Fig. 3A), and bedforms with more continuous and linear crestlines occur Fig. 10B. In the distal part of the LTR, the dune field is comprised of 13 large low-amplitude dunes, with many smaller scale dunes superimposed (Fig. 11B). These large low-amplitude dunes have $H = 1.3$ m and $L = 131$ m, are nearly symmetrical and have no discernable slip-faces (Fig. 11). The superimposed dunes are nearly as high ($H = 0.48$ m) as the large low-amplitude dunes, but are much shorter in length ($L = 7.8$ m). Both scales of dunes are persistent across a wide range of flows, having been recognized during other single beam surveys at high and low flow.

Bedform size and scaling

Figures 12 and 13 show distributions of dune height (H) and length (L) for each section of the

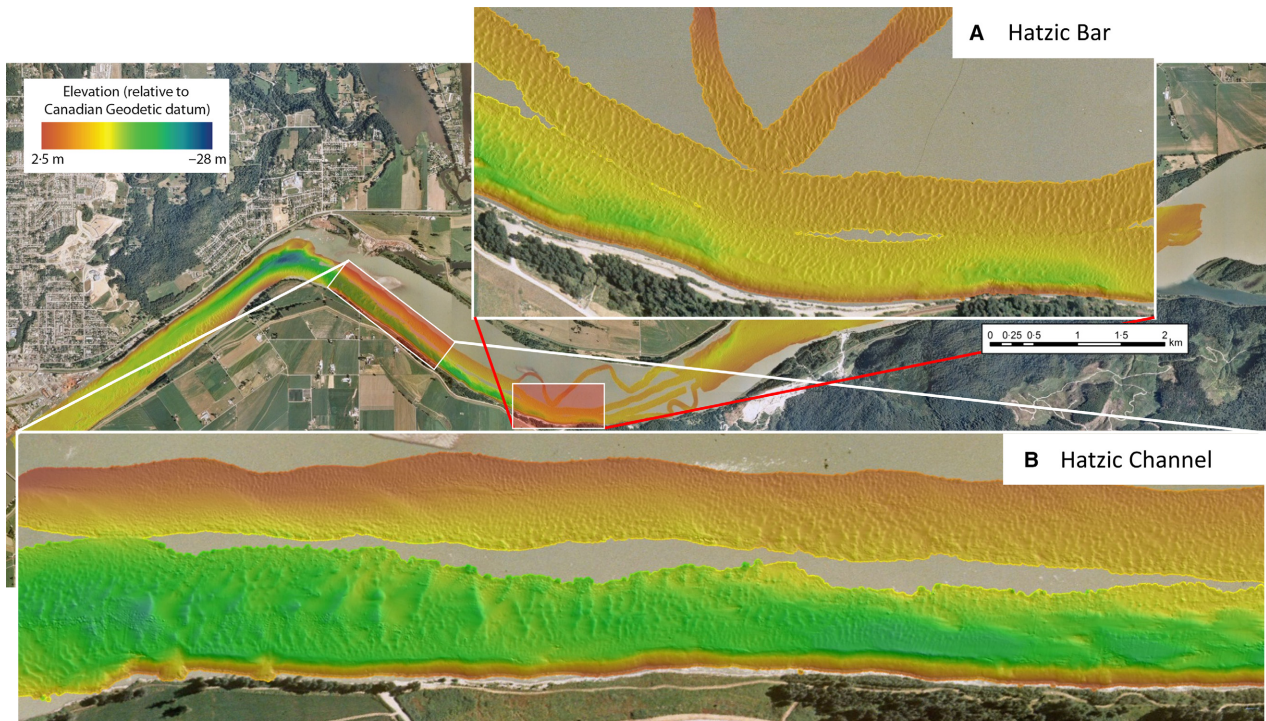


Fig. 9. (A) Laterally continuous bedforms on Hatzic Bar and (B) bedforms developing from a plane bed in Hatzic Channel. Elevation scale for insets are the same as the base map. Flow is from right to left.

river; statistical properties are summarized in Table 2. Dunes in the LTR are aggregated together, but large low-amplitude dunes are separated from the distributions because they are distinctive. The median bedform heights \bar{H} in the UTR and LTR are nearly identical (0.41 m and 0.45 m, respectively): \bar{H} is somewhat larger on Hatzic Bar (0.58 m) and much larger in Hatzic Channel (0.78 m), due to local absence of the smaller bedforms that cover most other sections of the reach. Median lengths \bar{L} are between 7 m and 9 m, except in Hatzic Channel where $\bar{L} = 15$ m. There are fundamental differences between the distributions of the height and length of the bedforms in each section of the reach. For UTR and Hatzic Bar, the distributions of H and L are comparatively narrow (small standard deviation; Table 2), compared to the LTR and Hatzic Channel because of the absence of larger bedforms in the UTR and on Hatzic Bar. Bedform heights in LTR have a continuous distribution to 1.6 m (Fig. 13A) and long tails of the distributions. In addition to the 13 large low-amplitude dunes, there are 27 bedforms with $H > 1.6$ m in the LTR and three have heights between 4 m and 5 m. Lengths have a similarly long tail to the distribution, which is

continuous to 40 m (Fig. 14A). There are 21 bedforms with longer L . The distributions of bedforms in Hatzic Channel are similar (Figs 12C and 13C) but the long tails of the distributions are absent.

Figure 14A shows the relation between H and L . Flemming (1988) used a compilation of bedforms from fluvial and tidal environments to show that $H = 0.067L^{0.81}$ and that the maximum height for a given length is constrained by the relation $H_{\max} = 0.16L^{0.84}$. A more recent compilation from Bradley & Venditti (2017) of dunes in rivers and unidirectional flow flumes, that considered only reach-averaged values, indicates that $H = 0.051L^{0.77}$, meaning that H is smaller for a given L when only river dunes are considered. A least-squares linear regression through the data in Fig. 14A (not shown) revealed a similar a slope (0.74 ± 0.034), but a 43% larger intercept (0.090) than Bradley & Venditti (2017), indicating that, for a given length, these dunes are higher than the mean relation from Bradley & Venditti (2017). While there are a limited number of dunes that exceed the Flemming (1988) relation for H_{\max} , the vast majority of the dunes have lower heights for a given length than Flemming's H_{\max} relation would predict.

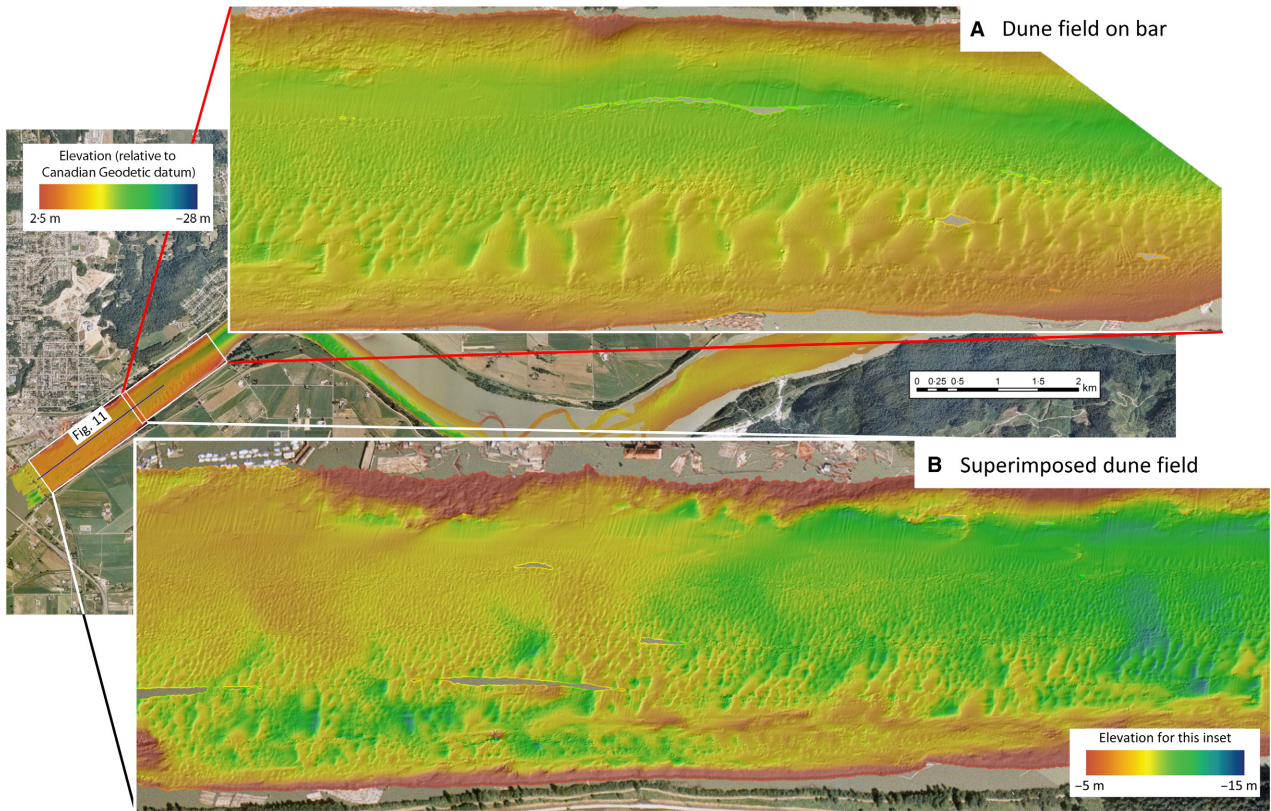


Fig. 10. (A) Depth-scaled dunes on a bar and (B) large, low-amplitude dunes with superimposed dunes in Lower Transitional Reach. Large, low-amplitude dunes identifiable as ridges of higher elevation that cross the channel. Elevation scale for insets are the same as the base map, unless otherwise indicated. The blue line indicates the transect extracted for Fig. 11, which runs through the centre of panels (A) and (B). Flow is from right to left.

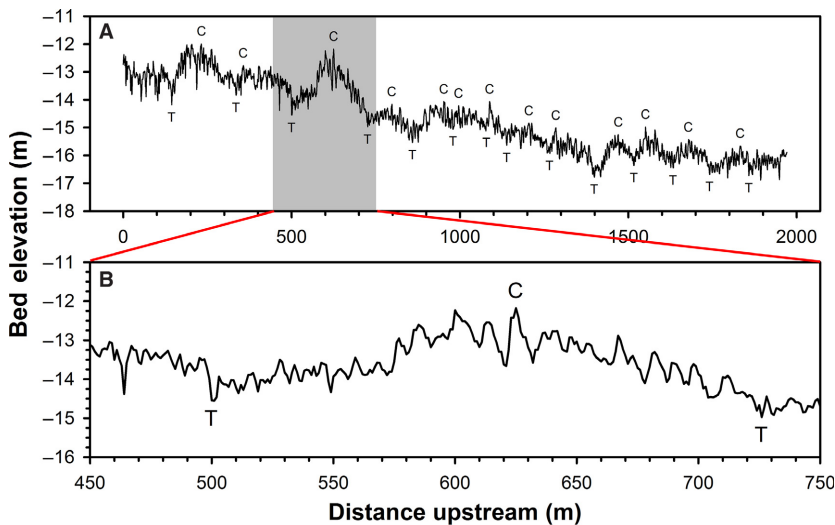


Fig. 11. Profile of large-scale, low-amplitude dune features shown in Fig. 10A and B: ‘C’ and ‘T’ are the crests and troughs, respectively, of individual bedforms that are superimposed by smaller features. Flow is from right to left.

The scaling between H and L is not affected by which section of the reach the dunes are in (Fig. 14A). There does not appear to be any alongstream pattern in the aspect ratio (L/H) of

the bedforms (Fig. 15A). Only the 13 large low-amplitude dunes in the LTR exhibit a different scaling. Excluding those dunes, mean aspect ratio $\bar{L}/H = 22$ and L/H ranges between 4 and

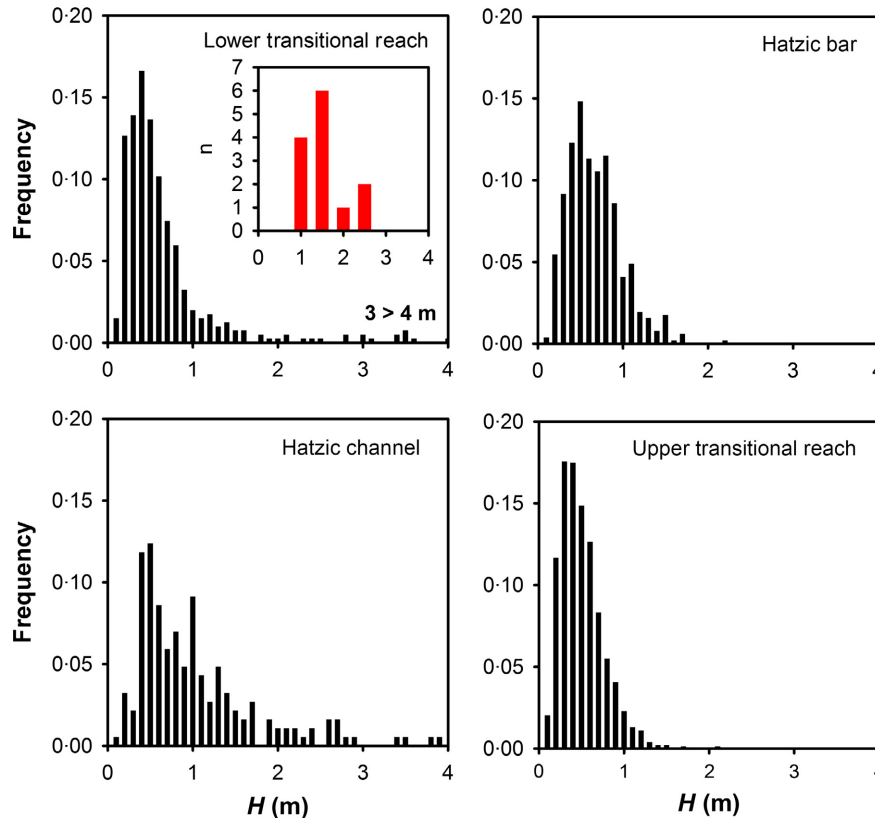


Fig. 12. Bedform height (H) histograms. Inset shows the distribution of large, low-amplitude dunes.

245, although 90% of the observations lie between 5 and 40 and only one dune exceeds 150. The large low amplitude dunes in the LTR have $\overline{L/H} = 112$.

It is widely held that H and L scale with flow depth (h) (cf. Allen, 1982; Bridge, 2003; Venditti, 2013). Excluding the large low-amplitude dunes in the LTR, the dune height scaling in this reach of the Fraser River ranges between ca $h/2.5$ and $h/100$ (Fig. 14B). The mean height scaling is $h/20$, with 90% of the variation below $h/60$, although the distribution has a long tail extending to $h/227$. Dune length scaling ranges between ca $5.0 h$ and $0.2 h$ with a mean scaling of $L = 0.9 h$ (Fig. 14C) and 90% of the variation below $1.5 h$. The L/h distribution has a long tail, which extends to $6.4 h$.

The vast majority of the dunes in the reach show no spatial variation in scaling, but there is some spatial variation in the scaling of the largest dunes (Fig. 15B and C). In Hatzic Channel and on the bar in the LTR, where there is abundant sand on the bed, some of the dunes exhibit height scaling between $2.5 h$ and $6.0 h$ (Fig. 15B) and length scaling between $1 h$ and

$5 h$ (Fig. 15C). The large low-amplitude dunes in the LTR exhibit different length scaling with depth, varying between $5 h$ and $16 h$ (Fig. 15B), but their height scaling with depth is within the variation observed for the rest of the dunes (Fig. 15C).

DISCUSSION

Do bedform patterns conform with increasing sediment supply to the bed?

Bedforms developed through the reach show that there is an increase in sand volume on the bed downstream, which constitutes an increase in the supply of sand to the bed. Bedforms in the Upper Transition Reach (UTR) are characteristic of the features formed in sand supply-limited conditions (Hersen *et al.*, 2002; Kleinhans *et al.*, 2002; Tuijnder & Ribberink, 2009; Grams & Wilcock, 2014; Venditti *et al.*, 2017). Barchan, barchanoid, isolated dunes, dunes with gaps in the troughs and linear, alongstream dune fields are all observed in the UTR. These observations

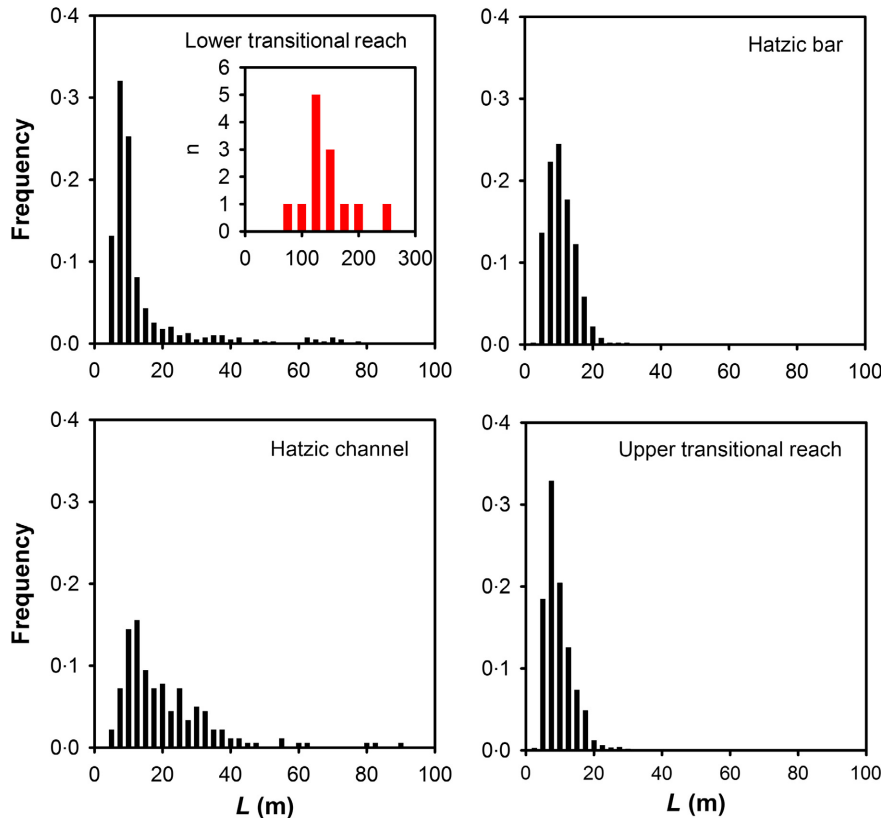


Fig. 13. Bedform length (L) histograms. Inset shows the distribution of large, low-amplitude dunes.

suggest that dunes in the UTR are developed on an immobile gravel bed in sand that is deformed into various bedforms depending on the local sand availability on the bed. Experimental work (e.g. Kleinhans *et al.*, 2002) suggests that in areas of very low sand availability on the bed – possibly the consequence of limited supply – isolated dunes form, and as sand supply progressively increases, the bed transitions from barchan and barchanoid dunes to a condition of nearly continuous dune coverage. In the UTR, the laterally continuous dunes maintain gaps with exposed gravel within the troughs through much of the dune field.

Hatzic Bar is a large sand bar with a veneer of gravel on the bar head (Venditti & Church, 2014). There is no apparent supply limitation on Hatzic bar, by definition an area of general sediment deposition. However the sand supply limitation from the UTR persists though Hatzic Channel insofar as a plane bed is exposed, likely composed of gravel-sized material, although a sample was extracted from Hatzic bend of the marine clay that underlies the Fraser River sediments. Nittrouer *et al.* (2011) have documented similar

exposures of semi-consolidated relict sediments in the lowermost Mississippi River. The plane bed through Hatzic Channel and Bend may be a similar type of exposure. Nevertheless, the sand coverage is discontinuous and where the thickness of sand increases, the bedforms grow in size.

In the Lower Transition Reach (LTR), most of the bed is covered by the same sized bedforms as in the UTR, however, the discontinuous sand bedforms associated with low sediment supply morphologies are absent. Along the southern bank, the bedforms grow to a substantial portion of the flow depth and are laterally continuous to the centre of the channel, where they terminate with developing gaps in the troughs where gravel is exposed. In the lower portion of the LTR, the bedforms acquire the type of low amplitude, long wavelength morphology with superimposed dunes that are common in large lowland river channels that are transport limited (Bradley & Venditti, 2017).

It is not clear from the present data why sand availability on the bed increases in the downstream direction. One possibility is that the bedload particle velocity decreases in the

Table 2. Properties of the bedform fields in each section of the transitional reach of the river. LTR, Lower Transition Reach; UTR, Upper Transition Reach.

	UTR	Hatzic Channel	Hatzic Bar	LTR
H minimum (m)	0.051	0.094	0.095	0.065
H maximum (m)	2.0	3.9	2.1	4.8
H mean (m)	0.46	0.98	0.62	0.65
H SD (m)	0.26	0.72	0.31	0.69
H median (m)	0.41	0.78	0.58	0.45
$H < 1$ m (%)	96	66	88	85
L minimum (m)	1.9	4.2	2.4	2.8
L maximum (m)	39	89	28	226
L mean (m)	8.5	19.5	9.4	15.9
L SD (m)	4.4	13.7	4.0	25.5
L median (m)	7.1	15.0	8.9	8.0
$L < 20$ m (%)	98	64	99	84

downstream direction, but that would require a decline in the shear stress. Another possibility for the downstream increase is sand coming out of suspension progressively through the reach. Venditti *et al.* (2015) explored suspended sediment dynamics through this reach of the river looking for downstream gradients in shear stress or suspended sediment flux that would support either of these hypotheses and did not find any.

Venditti *et al.* (2015) used spatially-resolved data to explore how far sediment could be carried in the reach. Those authors calculated a simple advection length scale that has the form:

$$A = \frac{h}{w_s} \bar{u} \quad (2)$$

where w_s is the settling velocity of a particular grain size and \bar{u} is the depth-averaged velocity. This advection length scale approximates the maximum distance downstream that a particle of given size can travel before interacting with the bed. Values of A for a range of sand sizes reveals that the median bed material can be suspended in the reach, but larger sizes cannot. Sizes < 0.180 mm can be transported for kilometres beyond the main channel spanning the GST, which is why those sizes make up $< 10\%$ of the bed material in the reach and are wash-load. The median size can be transported for a distance less than one channel width and coarser sizes beyond the main channel spanning the GST, which is why those sizes make up $< 10\%$ of the bed material in the reach and are wash-load. The median size can be transported for a distance less than one channel width and coarser sizes beyond the main channel spanning the GST, which is why those sizes make up $< 10\%$ of the bed material in the reach and are wash-load.

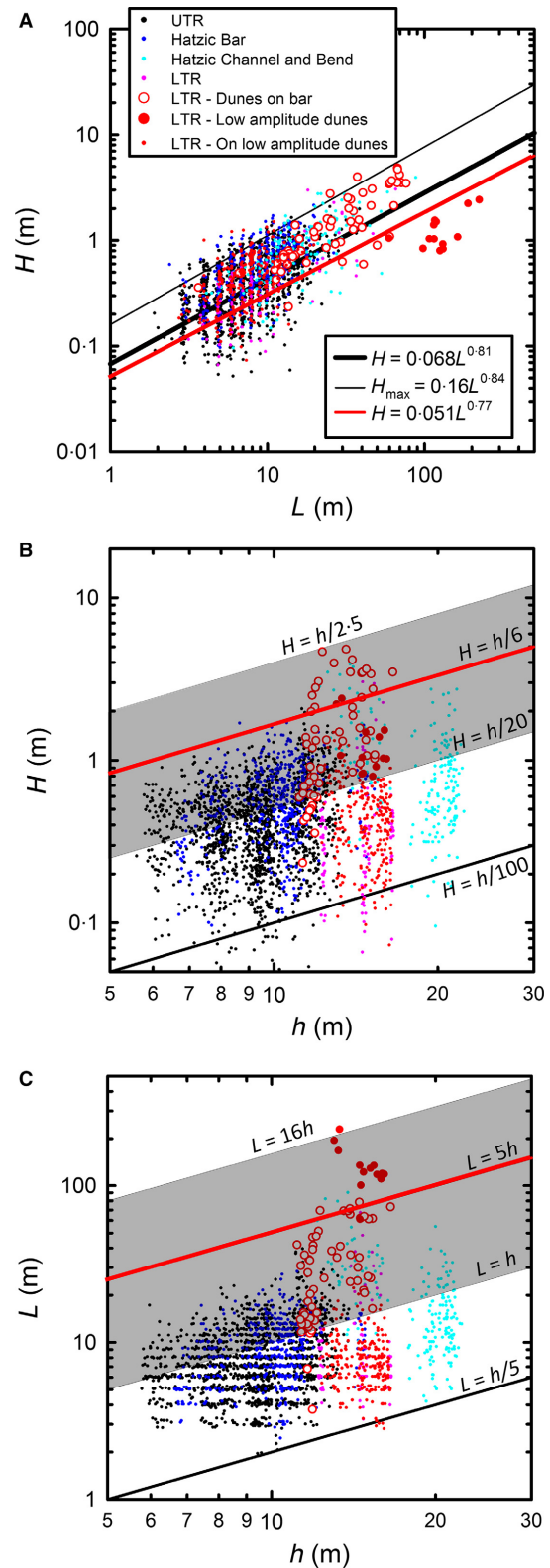


Fig. 14. Relation between: (A) bedform height (H) and length (L); (B) H and flow depth (h); and (C) L and h . The grey bands in (B) and (C) are range of scaling for river dunes from Bradley & Venditti (2017).

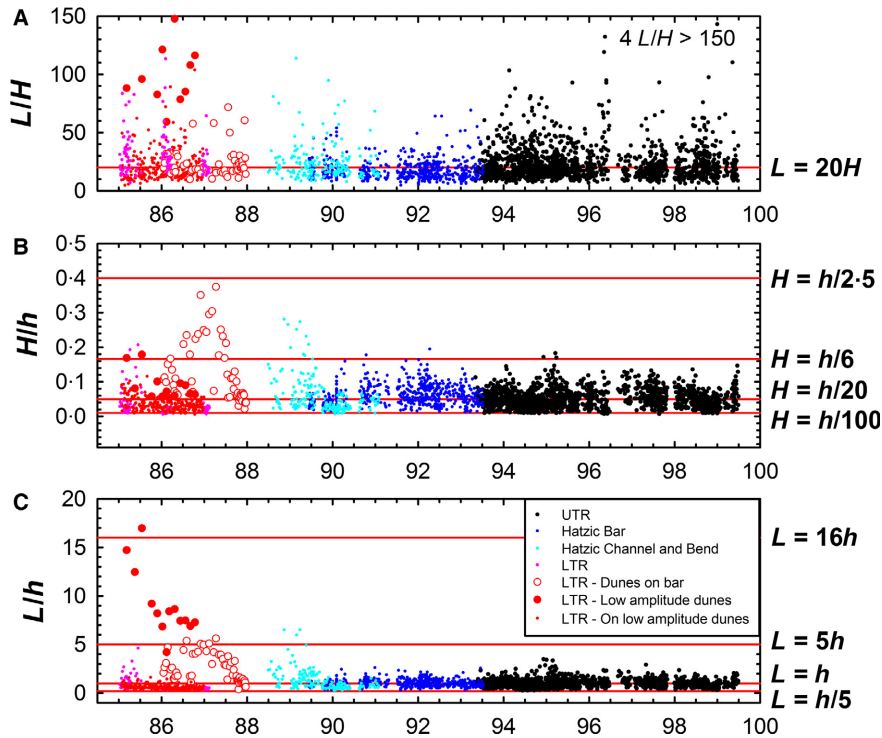


Fig. 15. Downstream change in dune: (A) aspect ratio (L/H); (B) height–depth scaling (H/h); and (C) length–depth scaling (L/h).

These calculations indicate immediate deposition of sand at the GST, rather than progressive suspension fallout of sand in the succeeding diffuse transition reach. Venditti *et al.* (2015) showed that up to 10 m of sand accumulates immediately downstream of the abrupt transition during low to moderate freshets and is periodically evacuated downstream during higher flows ($>10\,000\text{ m}^3\text{ sec}^{-1}$). Sand evidently deposits during low freshets and is redistributed during high freshets. The bedforms developed through the UTR are the result of sand diffusing downstream from the low freshet depositional zone at the termination of the cobble and gravel wedge (Fig. 2A) to the LTR. Evidently, the high freshet depositional zone is the LTR, which receives sand from the UTR and upstream. The observations herein followed a large flood flow when low freshet sand deposits had largely diffused downstream, creating the changes in bedform morphology from the supply-limited UTR to the transport-limited LTR.

Do dunes conform to conventional depth-scaling through the gravel–sand transition?

Dune height and length are often thought to scale with flow depth in rivers (see Bradley &

Venditti, 2017). Using dimensional analysis and a compilation of data from field and laboratory observations, Yalin (1964) argued that:

$$\frac{H}{h} = \frac{1}{6} \left(1 - \frac{\tau_c}{\tau} \right) \quad (3)$$

where τ is the boundary shear stress and τ_c is the stress required to entrain bed sediment. In most sand bedded rivers, the entrainment threshold is greatly exceeded and the ratio of shear stresses in the Yalin (1964) relation approaches zero. As a result, the relation was subsequently simplified to $H = h/6$ (cf. Allen, 1978). Yalin (1964) also used a data compilation to show that $L = 5h$. These relations are widely used in palaeo-environmental reconstructions and estimates of roughness in rivers.

Bradley & Venditti (2017) explored the depth scaling of dunes using a compilation of all available reach-averaged dune dimensions and flow depth for rivers and unidirectional flow flumes. Those authors found that dune dimensions do increase with flow depth, but the relation is not well defined. There is an order of magnitude variability in both dune H and L for any given h . Height ranged between $h/2.5$ and $h/20$ while

lengths ranged between 1 h and 16 h . Other data compilations that include data from rivers, estuaries and marine environments (cf. Allen, 1982) have established similar limits on dune dimensions, indicating that there are limits on how high a dune can get in a flow, but the size that emerges can be much less than that limit. Bradley & Venditti (2017) identified a scaling break in the height of dunes so that in shallow flows, dunes are generally higher than $h/6$, and in deeper flows, dune heights are less than $h/6$. Nevertheless, the order of magnitude variability in H and L for a given h persists.

The observations of this study do not conform to the conventional scaling attributed to Yalin (1964). In fact, no relation between dune dimensions and flow depth is found. As in previous data compilations, dunes do not grow larger in the flow than $h/2.5$ (Fig. 14B), suggesting that this may be the maximum dune height that can be achieved in a river. Dunes are observed with lengths greater than 16 h , but only marginally so (Fig. 14C). However, the conventional lower limits to the variability observed in previous data compilations do not apply to the present data set. Dunes with heights less than $h/20$ comprise 54% of these observations; dunes with lengths less than 1 h comprise 65% of the observations. These patterns emerge even if dunes superimposed on the large, low-amplitude dunes in the LTR are excluded.

What controls the height and length of supply-limited dunes?

The lack of a relation between flow depth and dune dimensions as well as the absence of a lower limit to dune size are curious results. It could be argued that dunes through the reach did not achieve equilibrium dimensions at the time of the present observations. However, these observations were made after an extended period of high flow and on the waning limb of the annual freshet, so this seems unlikely. If the conventional scaling is applied, then the dunes would be larger than one-sixth of the flow depth as water levels decline. Furthermore the appearance of large dunes on the bar in the LTR and in Hatzic Channel, approaching Hatzic Bend suggests that high flows persisted for long enough to develop larger dunes. However they did not appear in the UTR or the upstream end of Hatzic Channel where sand availability on the bed was limited.

It could be argued that the bedforms in the UTR and Hatzic Channel are limited by some boundary layer thickness other than flow depth

(e.g. Jackson, 1975). Unfortunately, the physical mechanism that would lead to such a limitation has not been fully elucidated. The limit of a boundary layer, and hence its thickness, is traditionally defined by the point in the flow where turbulence shifts from anisotropic to isotropic, as it does at the top of the atmospheric boundary layer (Oke, 1978). Flows in alluvial rivers are too shallow for a classical boundary layer to fully develop; they are always depth-limited (Nowell & Church, 1979) because macroturbulence mixes fluid through the full water column, particularly over dunes (Jackson, 1976; Kostaschuk & Church, 1993; Bradley *et al.*, 2013). Nevertheless, an internal boundary layer may develop at the roughness transition at the GST, but relations for growth of boundary layers downstream of a roughness transition (e.g. Wood, 1982) predict that a boundary layer developed at a roughness transition occurring at the GST would be equivalent to the flow depth within one channel width in the Fraser River. There does not appear to be any candidate boundary layer scales that would limit the height of dunes for more than 10 km in this reach of the Fraser River.

A more likely candidate for limiting the size of dunes in this reach of the Fraser River is the scarcity of sand. The only place where the dunes grow to consistently exist within the range defined by previous compilations (Allen, 1982; Bradley & Venditti, 2017) is where the bed is entirely sand in the LTR. It is likely that the diminutive dunes in the UTR and through Hatzic Channel are small because the sand availability is not sufficient to support larger dunes. Furthermore, the persistent gaps in the troughs of the diminutive dunes may limit the interaction of individual bedforms that leads to their coalescence and growth, and might also generate a local turbulence structure that can influence the geometry of the succeeding bedform. This hypothesis needs to be tested experimentally where accurate measurements of flow at scales below the bedform size are possible.

There is some previous work that shows that barchan dunes in the Rhine River can grow to a substantial proportion of the flow depth (cf. Carling *et al.*, 2000). This would suggest that supply limitation on the bed is not the sole control on dune dimensions. In the Fraser River, there is increasing sand availability on the bed moving downstream from the GST, which permits increasing dune height and length. Over some long lengths, which appear to exist in the Rhine

River, perhaps all of the small bedforms would coalesce into just a few large dunes. That does not happen in the Fraser River where there is a short length before the supply limitation on the bed disappears.

Ultimately, what controls the height and length of dunes in rivers is not fully understood (Bradley & Venditti, 2017). There are many theories, but none have been tested critically. Recent experimental work supports the idea that transport stage exerts a fundamental control on dune height and length (Bradley & Venditti, 2019). The experimental work of Kleinhans *et al.* (2002), summarized in Fig. 1, appears to support this idea for supply limited conditions. The observations of this study confirm that sediment supply to the bed plays a significant role in setting patterns and dimensions of bedforms in rivers.

CONCLUSIONS

The patterns, dimensions and depth-scaling of sandy bedforms through the diffuse gravel–sand transition (GST) of the Fraser River were examined. Bed topography was mapped with a multi-beam echo sounder immediately following an annual freshet flow peak that had a return period of 12 years. This flood provided an exceptional opportunity to examine the patterns of bedforms that develop when local sand availability on the bed is less than the volume required to cover the bed, and the change in bedforms from such supply-limited to transport-limited conditions in the downstream direction. The results show that:

1 The pattern of bedforms conforms with conceptual models of supply-limited bedforms, derived largely from laboratory experiments (e.g. Kleinhans *et al.*, 2002).

2 Near the channel spanning gravel–sand transition, trains of transverse dunes formed on locally thick, linear deposits of sand, analogous to sand ribbons with superimposed small-scale bedforms, barchan and barchanoid dunes, and dunes with gaps in the trough are observed. Further downstream, dunes approaching a substantial fraction of the flow depth, laterally-continuous dunes and large, low-amplitude, nearly-symmetrical dunes with smaller superimposed features are observed, that are characteristic of transport-limited conditions.

3 The conventional scaling of dune dimensions with flow depth does not emerge in the present data set in the supply-limited sections of the

reach. A substantial proportion of the dunes are below the depth-scaling ranges derived from compilations of dune observations in rivers.

The results suggest that sediment supply plays an important role in setting the height and length of dunes where local sand supply on the bed is less than the transport capacity. What ultimately controls the height of dunes is not presently clear; however, local sediment availability on the bed appears to be an important consideration.

ACKNOWLEDGEMENTS

This work was supported by Natural Sciences and Engineering Research Council (NSERC) Discovery Grants to JGV and MC; JAN and MAA acknowledge the Jackson School of Geosciences for financial support. This manuscript benefited from discussions with David Mohrig and Ryan Bradley, and constructive reviews from Paul Carling and Maarten Kleinhans. Technical support and field assistance were kindly provided by Dan Duncan (University of Texas at Austin). All data presented in this paper are freely available from the corresponding author (JGV) or the SFU Research Data Repository (<https://doi.org/10.25314/98aeed01-3c5c-45a3-987c-cb7f73ef4202>).

REFERENCES

- Allen, J.R.L. (1968) *Current Ripples; Their Relation to Patterns of Water and Sediment Motion*. North-Holland Publishing Company, Amsterdam, the Netherlands, 433 pp.
- Allen, J.R.L. (1978) Computational methods for dune time-lag: calculations using Stein's rule for dune height. *Sed. Geol.*, **20**, 165–216.
- Allen, J.R.L. (1982) *Sedimentary Structures: Their Character and Physical Basis*, vol. 1. Elsevier, Amsterdam, the Netherlands, 593 pp.
- Attard, M.A., Venditti, J.G. and Church, M. (2014) Suspended sediment transport in Fraser river at mission, British Columbia: New observations and comparison to historical records. *Can. J. Water Resour.*, **39**, 1–14.
- Bagnold, R.A. (1941) *The Physics of Blown Sand and Desert Dunes*. Methuen, London, UK, 265 pp.
- Bradley, R.W. and Venditti, J.G. (2017) Reevaluating dune scaling relations. *Earth-Sci. Rev.*, **165**, 356–376.
- Bradley, R.W. and Venditti, J.G. (2019) Transport scaling of dune dimensions in shallow flows. *J. Geophys. Res. Earth Surf.*, **124**, 526–547.
- Bradley, R.W., Venditti, J.G., Kostaschuk, R.A., Church, M., Hendershot, M. and Allison, M.A. (2013) Flow and sediment suspension events over low-angle dunes: Fraser Estuary, Canada. *J. Geophys. Res. Earth Surf.*, **118**, 1693–1709.
- Bridge, J.S. (2003) *Rivers and Floodplains: Forms, Processes, and Sedimentary Record*. John Wiley & Sons, Malden, MA, 491 pp.

- Carling, P.A., Gözl, E., Orr, H.G. and Radecki-Pawlik, A. (2000) The morphodynamics of fluvial sand dunes in the River Rhine, near Mainz, Germany. I. *Sed. Morphol. Sed.*, **47**, 227–252.
- Carling, P.A., Radecki-Pawlik, A., Williams, J.J., Rumble, B., Meshkova, L., Bell, P. and Breakspear, R. (2005) The morphodynamics and internal structure of intertidal fine-gravel dunes: Hills Flats, Severn Estuary, UK. *Sed. Geol.*, **183**, 159–179.
- Church, M. (2005) Bed material transport and the morphology of alluvial river channels. *Annu. Rev. Earth Planet. Sci.*, **34**, 325–354.
- Ernstsen, V.B., Noormets, R., Winter, C., Hebbeln, D., Bartholomä, A., Flemming, B. and Bartholdy, J. (2005) Development of subaqueous barchanoid-shaped dunes due to lateral grain size variability in a tidal inlet channel of the Danish Wadden Sea. *J. Geophys. Res. Earth Surf.*, **110**, F04S08, 1–13.
- Flemming, B.W. (1988) Zur klassifikation subaquatischer, stromungstrans versaler transportkörper. *Boch. Geol. U. Geotchn. Arb.*, **29**, 44–47 [in German].
- Franzetti, M., Le Roy, P., Delacourt, C., Garlan, T., Cancouet, R., Sukhovich, A. and Deschamps, A. (2013) Giant dune morphologies and dynamics in a deep continental shelf environment: example of the banc du four (Western Brittany, France). *Mar. Geol.*, **346**, 17–30.
- Grams, P.E. and Wilcock, P.R. (2014) Transport of fine sediment over a coarse, immobile riverbed. *J. Geophys. Res. Earth Surf.*, **119**, 188–211.
- Ham, D.G. (2005) *Morphodynamics and sediment transport in a wandering gravel-bed channel: Fraser River, B.C.* Ph.D. thesis, The University of British Columbia, Vancouver B.C., 210 pp.
- Hersen, P., Douady, S. and Andreotti, B. (2002) Relevant length scale for barchan dune. *Phys. Rev. Lett.*, **89**, 264301.
- Hickin, E.J. (1979) Concave-bank benches on the Squamish River, British Columbia, Canada. *Can. J. Earth Sci.*, **16**, 200–203.
- Jackson, R.G. (1975) Hierarchical attributes and a unifying model of bed forms composed of cohesionless material and produced by shearing flow. *GSA Bull.*, **86**, 1523–1533.
- Jackson, R.G. (1976) Sedimentological and fluid-dynamic implications of the turbulence bursting phenomenon in geophysical flows. *J. Fluid Mech.*, **77**, 531–560.
- Kenyon, N.H. and Stride, A.H. (1967) The crest length and sinuosity of some marine sand waves. *J. Sed. Petrol.*, **38**, 255–258.
- Kleinhans, M.G., Wilbers, A.W.E., De Swaaf, A. and Van Den Berg, J.H. (2002) Sediment supply-limited bedforms in sand-gravel bed rivers. *J. Sed. Res.*, **72**, 629–640.
- Kostaschuk, R.A. and Church, M.A. (1993) Macroturbulence generated by dunes: Fraser River, Canada. *Sed. Geol.*, **85**, 25–37.
- Lamb, M.P. and Venditti, J.G. (2016) The grain size gap and abrupt gravel-sand transitions in rivers due to suspension fallout. *Geophys. Res. Lett.*, **43**, 3777–3785.
- Lancaster, N. (1995) *Geomorphology of Desert Dunes*. Routledge, London, UK, 290 pp.
- Lonsdale, P. and Malfait, B. (1974) Abyssal dunes of foraminiferal sand on the Carnegie Ridge. *GSA Bull.*, **85**, 1697–1712.
- Lonsdale, P. and Spiess, F.N. (1977) Abyssal bedforms explored with a deeply towed instrument package. *Mar. Geol.*, **23**, 57–75.
- McCulloch, D.S. and Janda, R.J. (1964) Subaqueous river channel barchan dunes. *J. Sed. Petrol.*, **34**, 694.
- McLean, D.G. (1990) *Channel instability on lower Fraser River* Ph.D. thesis, The University of British Columbia, Vancouver B.C., pp. 290.
- McLean, D.G., Church, M. and Tassone, B. (1999) Sediment transport along lower Fraser River. 1. Measurements and hydraulic computations. *Water Res. Res.*, **35**, 2533–2548.
- Nittrouer, J.A. (2013) Backwater hydrodynamics and sediment transport in the lowermost Mississippi River Delta: implications for the development of fluvial-deltaic landforms in a large lowland river, in *Deltas: landforms, Ecosystems, and Human Activities*. G. Young and G. M. E. Perillo, editors. *IAHS Publ.*, **358**, 48–61.
- Nittrouer, J.A., Mohrig, D., Allison, M.A. and Peyret, A.B. (2011) The Lowermost Mississippi River: a mixed bedrock-alluvial channel. *Sedimentology*, **58**, 1914–1934.
- Nowell, A.R.M. and Church, M. (1979) Turbulent flow in a depth-limited boundary layer. *J. Geophys. Res. Earth Surf.*, **84**, 4816–4824.
- Oke, T.R. (1978) *Boundary Layer Climates*. Methuen and Co., London, UK, 435 pp.
- Parker, G. and Cui, Y. (1998) The arrested gravel front: stable gravel-sand transitions in Rivers Part 1: simplified analytical solution. *J. Hydraul. Res.*, **36**, 75–100.
- Reson Inc. (2009), *SeaBat 7101 High-Resolution Multibeam Echosounder System Operator's Manual*, Denmark, 168 pp.
- Tuijnder, A.P. and Ribberink, J.S. (2012) Experimental observation and modelling of roughness variation due to supply-limited sediment transport in uni-directional flow. *J. Hydraul. Res.*, **50**, 506–520.
- Tuijnder, A.P., Ribberink, J.S. and Hulscher, S.J.M.H. (2009) An experimental study into the geometry of supply-limited dunes. *Sedimentology*, **56**, 1713–1727.
- Venditti, J.G. (2013) Bedforms in sand-bedded rivers. In: *Treatise on Geomorphology, Fluvial Geomorphology* (Eds J.F. Shroder (Editor-in-Chief) and E. Wohl (Volume Editor)), vol. **9**, pp. 137–162. Academic Press, San Diego, CA.
- Venditti, J.G. and Church, M. (2014) Morphology and controls on the position of a gravel-sand transition: Fraser River, British Columbia'. *J. Geophys. Res. Earth Surf.*, **119**, 1959–1976.
- Venditti, J.G., Domarard, N., Church, M. and Rennie, C.D. (2015) Sediment dynamics through an abrupt gravel-sand transition. *J. Geophys. Res. Earth Surf.*, **120**, 943–963.
- Venditti, J.G., Nelson, P.A., Bradley, R.W., Haught, D. and Gitto, A.B. (2017) Bedforms, structures mobile patches and sediment supply in gravel-bedded rivers. In: *Gravel-Bed Rivers: Process and Disasters* (Eds D. Tsutsumi and J.B. Laronne), pp. 439–466. Wiley, Chichester, UK.
- Williams, J.J., Carling, P.A. and Bell, P.S. (2006) Dynamics of intertidal gravel dunes. *J. Geophys. Res.*, **111**, C06035.
- Wood, D.H. (1982) Internal boundary layer growth following a step change in surface roughness. *Bound. Lay. Meteorol.*, **22**, 241–244.
- Wynn, R.B., Masson, D.G. and Bett, B.J. (2002) Hydrodynamic significance of variable ripple morphology across deep-water barchan dunes in the Faroe-Shetland Channel. *Mar. Geol.*, **192**, 309–319.
- Yalin, S.M. (1964) Geometric properties of sand waves. *J. Hydraul. Div.*, **90**(HY5), 105–120.

Manuscript received 11 July 2017; revision accepted 13 March 2019